Theoretical Study of the Reaction $CH(X^2\Pi) + NO(X^2\Pi)$. 3. Determination of the Branching Ratios

N. Marchand, J. C. Rayez,* and S. C. Smith†

Laboratoire de Physicochimie Théorique, URA 503/CNRS, Université Bordeaux 1, Domaine Universitaire, 33405 Talence Cedex, France

Received: November 11, 1997; In Final Form: February 2, 1998

In this paper, which is the third of a series devoted to the title reaction, we present theoretical calculations of branching ratios for the product channels involved in the reaction. In the first paper of this series (Marchand, N.; Jimeno, P.; Rayez, J. C.; Liotard, D. *J. Phys. Chem.* **1997**, *101*, 6077.), we explored the topology of the lowest triplet potential energy surface determined with sophisticated ab initio methods and proposed several reaction paths connecting the reactants to the products. We have used these results to determine the branching ratios using two methods based on multichannel Rice−Ramsperger−Kassel−Marcus (RRKM) calculations: a μVTST/RRKM (μVTST = microcanonical variational transition state theory) method developed by one of us and an ACIOSA/RRKM (ACIOSA = adiabatic capture model using the infinite order sudden approximation) method dealing with a capture rate constant calculation (Marchand, N.; Stoecklin, T.; Rayez, J. C. To be submitted, of this series). Our present results reveal that, at 300 K, HCN + O is the major product channel involved in the reaction (72.0%), the other branching ratios being 13.9% for NCO + H, 8.2% for CO + NH, 3.3% for CNO + H, and 1.4% for CN + OH. All the others channels contribute for less than 1% each. These theoretical results are in agreement with the results of several experimental studies, especially those very recently obtained in our laboratory by Bergeat et al. Moreover, we observe no significant temperature dependence of the branching ratios.

I. Introduction

The methylidyne (CH) radical is one of the most important intermediates in combustion chemistry and is a highly reactive radical in planetary atmospheres.[1] Particularly, the reaction of the CH radical with NO is believed to play a crucial role in the overall reburning mechanism, because it provides a way to minimize emission from combustion processes producing NO_x atmospheric polluants. Hence, the determination of the relevant branching ratios is required to increase our knowledge about the NO reburning processes. Several kinetic studies of this reaction with various techniques have been reported.[2] All agree in their estimates of the total bimolecular rate constant of disappearance of CH and NO, yielding k (300 K) $\approx 2.0 \times 10^{-10}$ cm^3 molecule^{-1} s^{-1}. Furthermore, all experimental studies reveal no significant temperature dependence of this global rate constant over the large range [13−3790 K]. However, very little is known about the rate constants for formation of the different possible products at room temperature. This reaction is also likely to occur in interstellar chemistry, since the global rate constant of disappearance of reactants approaches the gas kinetic limit. Moreover, the molecule HNCO has recently been detected in the galactic center.[3,4]

Experimentally, several groups have reported an estimation of the product branching ratios for this reaction. In shock tube experiments, Dean et al.[2e] used near-UV laser absorption to estimate an upper limit of product branching ratios for the CO + NH and CN + OH channels in the temperature range 2600−3800 K. From the yield of NH, it was concluded that the CO + NH channel contributes less than 10% to the global rate constant. The measurement of the OH yield suggests that the product channel CN + OH also plays a minor role (certainly less than 30% and probably even less than 10%), since no CN radicals were detected in a significant amount. Dean et al. suggested that HCN + O is the major reaction product channel. Using laser induced fluorescence spectroscopy, Okada et al.[2f] estimated that the products CN + OH should participate less than 20% and the products CO + NH less than 15% at room temperature. Bozzelli et al.,[5] using a quantum version of the RRK method, predicted HCN + O to be the most probable products followed by HCO + N and NCO + H in that order. Consistent with all the previous experimental results, Takezaki and co-workers,[6] using a crossed-beam experiment, proposed the formation of HCN and/or OH as main products by a spectroscopic analysis. Although some divergences occur among the conclusions for the minor channels, experimental results concerning the branching ratios all agree that HCN is the most likely product. Lambrecht and Hershberger[7] have reported direct measurement of product yields in the CD + NO reaction at room temperature using time-resolved infrared diode laser spectroscopy detection. They used the deuterated species because HCN (which is presumed to be the major product of the reaction) absorbs outside the range of available infrared laser diodes. They have obtained the following branching ratios: 47.5 ± 12.2% for DCN + O, 18.8 ± 5.5% for NCO + D, an upper limit of <7.5% for CN + OD, and 33.7 ± 13.8% for the sum CO + ND and DCO + N channels. Lambrecht et al. in their study have reported no significant dependence of product branching ratio on NO pressure. In any case, all available data are in qualitative agreement that CN + OH product channel represent a very minor contribution to the total rate constant

* Corresponding author.
† Permanent address: Department of Chemistry, The University of Queensland, Brisbane Qld 4072, Australia.

S1089-5639(98)00159-5 CCC: $15.00
Published on Web 04/22/1998

TABLE 1: Experimental Values of Some Branching Ratios of Product Channels of the Reactions CH + NO and CD + NO Determined at 300 K by Several Groups Other than Bergeat et al.[8]

products	Dean et al.[2e]	Okada et al.[2f]	Lambrecht et al.[7]
CH + NO			
HCN + O	major		
NCO + H		major	
HCO + N			
CO + NH	<10%	15%	
CN + OH	<30%	0.2% for CN ≈20% for OH	
CD + NO			
DCN + O			47.5 ± 12%
NCO + D			18.8 ± 5.5%
DCO + N and CO + ND			33.7 ± 13.8%
CN + OD			<7.5%

and that HCN seems to be the major product. All these available experimental branching ratio determinations are gathered in Table 1.

Very recently, various kinetic aspects of this reaction have been studied experimentally in our laboratory by Bergeat et al.[8] They used a low-pressure (2 Torr He) fast-flow reactor where the CH radicals are produced by the reaction of bromoform $CHBr_3$ with potassium vaporized in a microfurnace ending into a nozzle.[9] In this way, since the CH + K reaction is endoergic, the source of CH radicals is "clean" and CH($X^2\Pi$) is formed in the lowest vibrational level. The overall rate constant has been measured by monitoring the decay of the CH radicals (NO being introduced in large excess), and they have obtained k (300 K) $\approx 1.9 \times 10^{-10}$ cm^3 molecule^{-1} s^{-1}. Moreover, this study is the first experimental study which reports branching ratios for the reaction involving hydrogen atom instead of deuterium atom (vide supra). Moreover, some diatomic products have been probed by laser induced fluorescence (LIF) or by chemiluminescence in the range of 120−800 nm. In particular, they found that, if the product channels CN + OH are actually formed, it is in very small amount. The originality of this study lies in the fact that the product branching ratios have been determined by atomic resonance fluorescence in a vacuum ultraviolet over the pathways yielding atoms. The branching ratios of the product channels associated with the formation of atoms O, H, and N are displayed in Table 2. At 300 K, HCO is assumed to be partially decomposed into H + CO, but Bergeat et al. do not know how. At any event, the amount of hydrogen atom recorded is certainely overestimated with respect to the quantity supplies by the channels leading to NCO + H and CNO + H. To simulate a realistic situation, Bergeat et al. have estimated the two extreme situations in which HCO and HOC are fully dissociated or not at all, to determine the range in which the branching ratios lie. Then, the branching ratios, corresponding to the oxygen detection which comes from the participation of the product channels HCN + O and HNC + O, lies between 69 and 74%. Related to the formation of H atom coming from NCO + H, CNO + H, and HCO + N (HCO leading itself partially to CO + H), they obtain a value between 19 and 24%. The branching ratios for channels leading to nitrogen atom (i.e., HCO + N and HOC + N are around 7%).

The key issue in the theoretical determination of the rate constants and branching ratios is the capability of ab initio methods to determine the relevant potential energy surfaces (PESs) which play a role in the reaction. A complete exact determination of a four-atom PES is still out of reach. Nevertheless, the knowledge of some parts of the surface may be sufficient to extract valuable information concerning the densities and sums of states necessary to determine microcanonical rate constants. With regard to the title reaction, several ab initio calculations were performed 20 years ago on the singlet PES.[10] More recently, a density functional theory (DFT) study of the potential energy surfaces of singlet and triplet multiplicities of CHNO isomers, using the hybrid density functional B3LYP method to investigate the PES, has been carried out by Mebel et al.[11] We have also performed elaborate ab initio calculations (paper 1[12]) on the singlet and triplet PES using CASSCF/D95 and CASPT2/D95 approaches, both involving 10 electrons in 10 orbitals. It turns out that the triplet surface plays the major role in the reaction since; in contrast to the singlet surface, it does not seem to present any barrier along the entrance channel. One extra argument is that statistically the triplet surface contributes a factor of 3 relative to the singlet process. Moreover, although HCN appears to be the major product, the fact that no ^{1}D oxygen atom has been detected by Bergeat et al.[8] is a solid argument in favor of the dominant role of the triplet surface. From the analysis of the shape of the reaction paths obtained with these different ab initio approaches, we have found that the path leading to the exothermic formation of the products HCN + O is the one possessing the smallest number of molecular rearrangements involving intermediate wells with barriers much smaller than the average energy at 300 K. The pathways leading to the very exothermic product channels NCO + H and CO + NH are also thermodynamically favorable in the reaction but many more rearrangements are involved. These qualitative tendancies are consistent with the experimental findings.

Building on the results of our previous two papers (i.e., ab initio geometries of the relevant structures [H, C, N, O] involved in the different pathways[12] and a computed value for the capture rate constant)[13] we present in this paper a theoretical determination of the branching ratios for the different product channels involved in the reaction using two different approaches based on multichannel RRKM calculations. In section II, the two theoretical methodologies are summarized. The results are presented and discussed in relation to the available experimental data in section III. Section IV concludes.

II. Multichannel RRKM Calculations

The potential energy surface in the entrance channel of the HC + NO reaction is purely attractive, and hence it requires a detailed capture calculation which explicitly allows for the effects of both angular momentum and anisotropy in the PES which varies in magnitude as the fragments approach each other. We have implemented two different approaches for the determination of the microcanonical rate constant of the first step of the reaction (capture of CH by NO). Each of the approaches is then coupled with RRKM theory for the determination of product branching ratios. In the first approach, we use microcanonical variational transition state theory (μVTST) in conjunction with Rice−Ramsperger−Kassel−Marcus (RRKM) theory (referred to throughout as μVTST/RRKM). The second approach is based on an adiabatic capture model using the infinite order sudden approximation (ACIOSA, see paper 2[13]) also coupled with RRKM calculations for the other steps. This second approach is called ACIOSA/RRKM. Since, in the adiabatic capture theory, the possibility of redissociation back to reactants from the collision complex is neglected, the use of a result coming out from such an approach can only lead to an upper limit of the global rate constant of disappearance of the reactants. In paper 2,[13] we have reported the rate constants calculations with three capture methods: ACIOSA, ACPCSA,

TABLE 2: Experimental Values of Branching Ratios of Product Channels of the Reaction CH + NO at 300 K Obtained by Bergeat et al.[8] with Atomic Resonance Lamps (See Text)[a]

atom formed by the reaction CH + NO	if HCO and HOC are not dissociated at all	if HCO and HOC are completely dissociated into CO + H	average situation: HCO and HOC are dissociated at 50%
O atom	74 ± 11% (HCN + O and HNC + O)	69 ± 10% (HCN + O and HNC + O)	72 ± 10%
H atom	19 ± 8% (NCO + H and CNO + H)	24 ± 5% (NCO + H, CNO + H, and CO + H + N)	21 ± 10%
N atom	7 ± 3% (HCO + N and HOC + N)	7 ± 3% (CO + H + N)	7 ± 3%

[a] These quantities concern all the channels leading to the formation of O, H, and N atoms. Two situations have been simulated: (i) the case where HCO and HOC are assumed to be totally dissociated and (ii) the case where HCO and HOC are not dissociated at all. An average situation assuming 50% of dissociation of HCO and HOC is proposed.

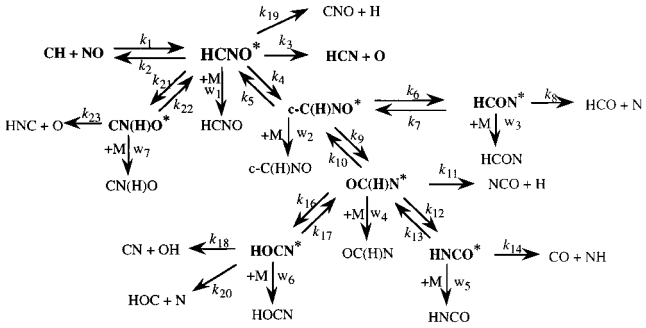

Figure 1. Different chemical equilibria and channels involved in the multichannel RRKM calculations for the CH + NO reaction. The reaction paths are refereed as those presented in paper 1.[12] The symbol "*" represents internal excitation of intermediates.

and ACGCSA for the title reaction. As expected, these three approaches overestimate the experimental value of Bocherel et al.,[14] provided that no damping function is introduced to attenuate the role of the dispersion term at short ranges (in other words, the intermolecular potential is used crudely). *A priori*, any of the calculated microcanonical rate constants $k(E)$ obtained from the three capture methods could be used to determine the branching ratios of the CH + NO reaction. But, since we show that the ACIOSA calculations gave results closer to the experimental results of Bocherel than the two other methods (without damping function), we have decided to keep the $k(E)$ ACIOSA value in the further determination of the branching ratios.

A. The μVTST/RRKM Model. Analagous to a recent study of the NH_2 + NO reaction by Diau and Smith,[15] we have derived and implemented the microcanonical steady-state RRKM equations appropriate to the mechanism for formation of each set of products, with explicit resolution of the total angular momentum through all steps prior to the final thermal averaging. The unified statistical model of Miller[16] has been used with success in some cases,[17] but in the present case we have not used it since we have deep wells and so it would be unlikely to affect the results. Some other approaches have been already used like the one presented by W. Hase et al.[17,18] and S. Klippenstein[19] involving direct summation over the orbital and reactants rotational angular momenta leading to chemical association. In our case, we used a different way of summing which in no way affects the results. The multiple-well multichannel RRKM calculation for the CH + NO reaction is performed according to the mechanistic scheme, presented in Figure 1, based on the results of paper 1[12] (the same numbering of reactions and intermediates is used here).

The steady-state treatment for all the intermediates along the pathway to each product channel gives the (E,J)-specific branching probabilities. The thermally averaged rate constants for each channel are obtained by a Boltzmann average of these probabilities. The following equations give the thermal rate constants for each open channel involved in the reaction:

$$k_{\mathrm{HCN}}(T) = Q\sum_{J=0}^{\infty}(2J+1)\int \mathrm{d}E\,\frac{k_3(E,J)}{F(E,J)}W(E,J)\mathrm{e}^{-E/k_{\mathrm{B}}T} \quad (1)$$

$$k_{\mathrm{NCO}}(T) = Q\sum_{J=0}^{\infty}(2J+1)\int \mathrm{d}E\,\frac{k_{11}(E,J)D(E,J)E(E,J)}{F(E,J)} \times W(E,J)\mathrm{e}^{-E/k_{\mathrm{B}}T} \quad (2)$$

$$k_{\mathrm{HCO}}(T) = Q\sum_{J=0}^{\infty}(2J+1)\int \mathrm{d}E\,\frac{k_8(E,J)A(E,J)E(E,J)}{F(E,J)} \times W(E,J)\mathrm{e}^{-E/k_{\mathrm{B}}T} \quad (3)$$

$$k_{\mathrm{CO}}(T) = Q\sum_{J=0}^{\infty}(2J+1)\int \mathrm{d}E\,\frac{k_{14}(E,J)B(E,J)D(E,J)E(E,J)}{F(E,J)} \times W(E,J)\mathrm{e}^{-E/k_{\mathrm{B}}T} \quad (4)$$

$$k_{\mathrm{CN}}(T) = Q\sum_{J=0}^{\infty}(2J+1)\int \mathrm{d}E\,\frac{k_{18}(E,J)C(E,J)D(E,J)E(E,J)}{F(E,J)} \times W(E,J)\mathrm{e}^{-E/k_{\mathrm{B}}T} \quad (5)$$

$$k_{\mathrm{CNO}}(T) = Q\sum_{J=0}^{\infty}(2J+1)\int \mathrm{d}E\,\frac{k_{19}(E,J)}{F(E,J)}W(E,J)\mathrm{e}^{-E/k_{\mathrm{B}}T} \quad (6)$$

$$k_{\mathrm{HOC}}(T) = Q\sum_{J=0}^{\infty}(2J+1)\int \mathrm{d}E\,\frac{k_{20}(E,J)C(E,J)D(E,J)E(E,J)}{F(E,J)} \times W(E,J)\mathrm{e}^{-E/k_{\mathrm{B}}T} \quad (7)$$

$$k_{\mathrm{HNC}}(T) = Q\sum_{J=0}^{\infty}(2J+1)\int \mathrm{d}E\,\frac{k_{23}(E,J)Z(E,J)}{F(E,J)}W(E,J)\mathrm{e}^{-E/k_{\mathrm{B}}T} \quad (8)$$

$$k_{w_1}(T) = Q\sum_{J=0}^{\infty}(2J+1)\int \mathrm{d}E\,\frac{w_1}{F(E,J)}W(E,J)\mathrm{e}^{-E/k_{\mathrm{B}}T} \quad (9)$$

$$k_{w_2}(T) = Q\sum_{J=0}^{\infty}(2J+1)\int \mathrm{d}E\,\frac{w_2 E(E,J)}{F(E,J)}W(E,J)\mathrm{e}^{-E/k_\mathrm{B}T} \quad (10)$$

$$k_{w_3}(T) = Q\sum_{J=0}^{\infty}(2J+1)\int \mathrm{d}E\,\frac{w_3 A(E,J)E(E,J)}{F(E,J)}W(E,J)\mathrm{e}^{-E/k_\mathrm{B}T} \quad (11)$$

$$k_{w_4}(T) = Q\sum_{J=0}^{\infty}(2J+1)\int \mathrm{d}E\,\frac{w_4 D(E,J)E(E,J)}{F(E,J)}W(E,J)\mathrm{e}^{-E/k_\mathrm{B}T} \quad (12)$$

$$k_{w_5}(T) = Q\sum_{J=0}^{\infty}(2J+1)\int \mathrm{d}E\,\frac{w_5 B(E,J)D(E,J)E(E,J)}{F(E,J)}W(E,J)\mathrm{e}^{-E/k_\mathrm{B}T} \quad (13)$$

$$k_{w_6}(T) = Q\sum_{J=0}^{\infty}(2J+1)\int \mathrm{d}E\,\frac{w_6 C(E,J)D(E,J)E(E,J)}{F(E,J)}W(E,J)\mathrm{e}^{-E/k_\mathrm{B}T} \quad (14)$$

$$k_{w_7}(T) = Q\sum_{J=0}^{\infty}(2J+1)\int \mathrm{d}E\,\frac{w_7 C(E,J)Z(E,J)}{F(E,J)}W(E,J)\mathrm{e}^{-E/k_\mathrm{B}T} \quad (15)$$

with

$$A(E,J) = \frac{k_6(E,J)}{k_7(E,J) + k_8(E,J) + w_3} \quad (16)$$

$$B(E,J) = \frac{k_{16}(E,J)}{k_{17}(E,J) + k_{18}(E,J) + w_6 + k_{20}(E,J)} \quad (17)$$

$$C(E,J) = \frac{k_{16}(E,J)}{k_{17}(E,J) + w_6 + k_{18}(E,J) + k_{20}(E,J)} \quad (18)$$

$$D(E,J) = k_9(E,J)/[k_{10}(E,J) + k_{11}(E,J) + k_{12}(E,J) + k_{16}(E,J) + w_4 - k_{13}(E,J)B(E,J) - k_{17}(E,J)C(E,J)] \quad (19)$$

$$E(E,J) = k_4(E,J)/[k_5(E,J) + k_6(E,J) + k_9(E,J) + w_2 - k_7(E,J)A(E,J) - k_{10}(E,J)D(E,J)] \quad (20)$$

$$Z(E,J) = \frac{k_{21}(E,J)}{k_{22}(E,J) + w_7 + k_{23}(E,J)} \quad (21)$$

$$F(E,J) = k_2(E,J) + w_1 + k_3(E,J) + k_4(E,J) + k_{19}(E,J) + k_{21}(E,J) - k_5(E,J)E(E,J) - k_{22}(E,J)Z(E,J) \quad (22)$$

and

$$Q = \frac{g_\mathrm{e}}{hQ_\mathrm{CH}Q_\mathrm{NO}}\exp[-E^0/k_\mathrm{B}T] \quad (23)$$

The quantity $k_j(T)$ is the rate constant of the product channel j involved in the reaction and $k_{w_i}(T)$ is the stabilization rate constant of the excited species *i*. $W(E,J)$ represents the sum of states of the transition state along the entrance channel. In the definition of the Q quantity, E^0 is the energy difference between the zero-point level of the transition state structure and the separated reactants for process 1 at 0 K. In our case, $E^0 = 0$, since no barrier appears along the entrance channel. Then, $\exp[-E^0/k_\mathrm{B}T] = 1$. The quantities Q_CH and Q_NO are the partition functions of the reactants (electronic part and center of mass motion excluded), and g_e is the ratio between the electronic partition function of the collision complex (which is assumed to be 1) and the electronic partition function of the reactants, which is the product of the relevant terms for CH and for NO (i.e., $2 + 2\exp(-25.76/T)$ and $2 + 2\exp(-174.16/T)$, respectively). The temperature dependence arises from the spin−orbit splitting of the $^2\Pi$ levels of both fragments.[20] The microcanonical rate coefficient expressed as a function of total energy and angular momentum, is given by (see Figure 2 for the definition of the energies):

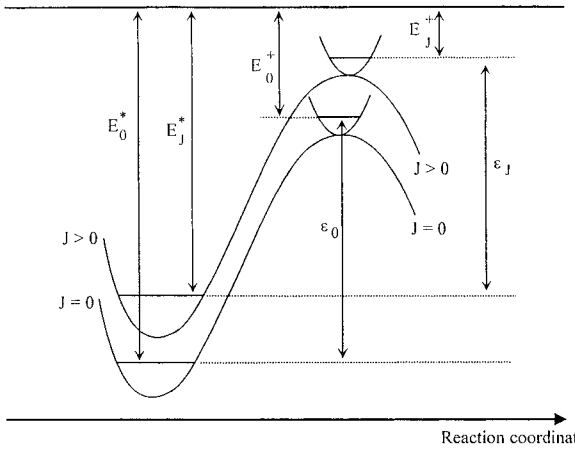

Figure 2. Illustration of the energy terminology used for an unimolecular reaction.

$$k_i(E_J^*, J) = \frac{W_i(E_J^* - \epsilon_J, J)}{h\rho_j(E_J^*, J)} \quad (24)$$

where $W_i(E_J^* - \epsilon_J, J)$ is the sum of states of the activated complex i {i = 2, 3, 4, 5, 6, 7, 9, 10, 21, 22, 23, 27, according to the numbering of the transition states introduced in ref 12}, $\rho_j(E_J^*, J)$ is the density of states at the energy E_J^* of the intermediate j {j = A, C, D, E, F, H, I, see ref 12 for the labeling of the complexes} and h is the Planck's constant. The determination of the sum of states $W_i(E_J^* - \epsilon_J, J)$ depends on the nature, tight or loose, of the transition state. The case of a loose transition state is encountered only once, along the entrance channel. All the other transition states are tight. The sum of states $W_i(E_J^* - \epsilon_J, J)$ for a tight transition state is calculated by the convolution of the vibrational and rotational sum of states counted with the Beyer−Swinehart algorithm.[21] The loose transition state corresponds to a large C−N distance between fragments CH and NO. In such a case, it is convenient to assume separability between the two stretching vibrations of CH and NO (conserved modes) and the four transition modes to evaluate $W_i(E_J^* - \epsilon_J, J)$, since $W_i(E_J^* - \epsilon_J, J)$ can then be simply written as a convolution of the transition mode sum of states and the conserved mode density of states. Due to the large C−N distance, we can assume that the CH and NO frequencies of stretching are the same as in the separated diatomic molecules. Among the four rotational degrees of freedom of CH and NO (which are the genuine transitional modes), three become hindered as the separated fragments approach each other, ultimately being transformed into vibrational modes in the collision complex. The fourth rotational degree of freedom becomes the K-rotational degree of freedom of the transition state assuming that the conformation of this

TABLE 3: Vibrational Frequencies and Rotational Constants (Both in cm^{-1}) Calculated at UHF/6-31G ab initio Level for Each Intermediate Involved in the Different Pathways[a]**

							rotational constants		
frequencies	ν_1	ν_2	ν_3	ν_4	ν_5	ν_6	*A*	*B*	*C*
HCNO (*A*)	582	704	1036	1206	1442	3410	4.047	0.448	0.404
DCNO	534	543	885	1122	1425	2517	4.137	0.39	0.363
c−C(H)NO (*C*)	990	1059	1167	1219	1563	3311	1.168	1.107	0.590
c−C(D)NO	833	913	996	1140	1542	2447	1.126	0.941	0.542
OC(H)N (*D*)	612	945	1131	1323	1703	3226	3.288	0.423	0.375
OC(D)N	605	803	954	1144	1685	2372	2.324	0.424	0.358
HNCO (*E*)	131	614	929	1237	1983	3686	4.951	0.392	0.367
DNCO	102	594	869	998	1979	2694	4.515	0.362	0.340
HOCN (*H*)	542	941	1072	1429	1442	4137	3.207	0.434	0.382
DOCN	526	704	981	1175	1438	3013	3.165	0.402	0.357
HCON (*I*)	529	763	1099	1356	1527	3127	3.214	0.467	0.408
DCON	511	580	1020	1239	1359	2298	3.135	0.424	0.374
CH	3029						14.724	14.724	
DH	2217						7.925	7.925	
NO	2243						1.78	1.78	

[a] Deuterated compounds are also presented on the row just below the hydrogenated ones. The letters *(X)* correspond to the label of the intermediates found in our theoretical study.[12]

transition state is a symmetric top. To determine the sum of states for this loose transition state, we have used the μVTST formalism developed by Smith.[22] In this approach, the loose transition state is located along the reaction coordinate by the variational criterion of minimizing the sum of states $W_i(E_J^* - \epsilon_J, J)$. The application of μVTST with rigorous incorporation of angular momentum constraints for this class of reactions was introduced by Wardlaw and Marcus[23] and further developed by Klippenstein.[24] Smith's work[22] showed a particularly efficient way to evaluate the transition mode sum of states, using classical analytic expressions for the momentum−space volume followed by a Monte Carlo integration over the internal angular configuration space. We used a simple model for the interaction potential for the entrance channel: the reaction coordinate was chosen to be the separation *R* between the atoms C and N which are forming the C−N bond in the first intermediate HCNO (formonitrile oxide, which is common to all the reaction paths). The radial dependence of the bonding interaction has been modeled by a pointwise potential calculated by ourselves using the CASPT2 ab initio method.[12] The anisotropy of the bonding potential is approximated by the angular part of the dipole−dipole interaction potential:[25]

$$V_{\text{anis}}(\theta_1,\theta_2,\phi) = (-2\cos\theta_1\cos\theta_2 + 2\sin\theta_1\sin\theta_2\cos\phi) \quad (25)$$

Tables 3 and 4 contain the vibrational frequencies and rotational constants, calculated at the UHF/6-31G** ab initio level, of all HCNO and DCNO isomers involved in the reaction paths (minima and saddle points). It is interesting to notice that all the four-atom structures reported in Tables 3 and 4 are quasi-symmetric tops. These data, coupled with the geometries of each stationary point, are necessary to calculate the densities and the sums of states which appear in formula 24.

The effective collision frequencies, $w_i = \beta_c Z_{LJ}$[M], where β_c is the collision efficiency, Z_{LJ} is the Lennard-Jones collision frequency, and [M] is the concentration of the gas bath M, were estimated with the Troe's collision model.[26] However, as the Lennard-Jones parameters for the molecules involved in all the reaction paths are not available in the literature, some were estimated by standard methods. Furthermore, we assumed that the collision frequency factor Z_{LJ} is the same for all the molecules, so we did the calculation only for the formonitrile oxide (HCNO) labeled *A* in the following equations. The

TABLE 4: Vibrational Frequencies and Rotational Constants (Both in cm^{-1}) Calculated at UHF/6-31Gab initio Level for Each Saddle Point Involved in the Different Reaction Paths[a]**

						rotational constants		
frequencies	ν_1	ν_2	ν_3	ν_4	ν_5	*A*	*B*	*C*
2	496	718	906	1585	3456	3.071	0.393	0.348
2D	453	545	750	1542	2568	3.033	0.354	0.317
3	944	1053	1244	1569	3562	1.198	1.088	0.570
3D	761	995	1219	1517	2666	1.186	0.902	0.512
4	517	1142	1209	1356	3362	1.670	0.635	0.477
4D	384	777	902	1389	2472	1.515	0.577	0.443
5	459	979	1381	1401	3046	2.630	0.404	0.351
5D	412	438	884	1073	2244	2.621	0.369	0.324
6	1046	1153	1284	1448	3255	1.294	0.792	0.506
6D	845	931	1138	1427	2400	1.074	0.777	0.472
7	345	731	1118	1356	2142	4.594	0.410	0.383
7D	314	649	1112	1347	1549	3.471	0.399	0.368
9	122	494	1115	2205	3622	4.077	0.333	0.308
8D	94	482	833	2204	2648	3.758	0.310	0.286
21	468	600	1273	1790	2487	5.293	0.398	0.371
21D	386	598	1272	1627	1957	4.070	0.389	0.355
22	298	448	910	1412	3996	2.424	0.399	0.343
22D	225	437	678	1411	2910	2.350	0.372	0.321

[a] The numbers n are the labels of the saddle points according to our theoretical study.[12] Deuterated structures are labeled as *n*D.

Lennard-Jones collision diameter $\sigma_{A-M} = (\sigma_A + \sigma_M)/2$ and the Lennard-Jones well depth $\epsilon_{A-M} = (\epsilon_{A-A}\,\epsilon_{M-M})^{1/2}$ were determined by Stiel and Thodos method[27] with the following expressions:

$$\sigma = 0.812(T_c/P_c)^{1/3} Z_c^{-13/15} \qquad \text{and}$$

$$(\epsilon/k) = 65.3\, T_c Z_c^{18/5} \quad (26)$$

where P_c is the critical pressure calculated by Riedel method,[27] Z_c is the critical compressibility factor estimated by García−Bárcena method,[27] V_c is the critical volume calculated by using Lydersen method,[27] and T_c the critical temperature was deduced from the previous calculated quantities by the relation: $T_c = P_c V_c/(RZ_c)$. The parameters obtained for the calculations of the effective collision frequencies w_i are listed in Table 5.

The total second-order rate constant for the CH + NO reaction is given by

$$k_{\text{tot}}(T) = \sum_j k_j(T) + \sum_i k_{w_i}(\text{T}) \quad (27)$$

TABLE 5: Lennard-Jones Parameters Calculated for the HCNO Molecule (Labeled *A*) Colliding with Helium (Labeled *M*) at Room Temperature and under 50 Torr Pressure

σ_A	4.4237 Å
$(\epsilon/k)_A$	257.881 K
σ_M	2.551 Å
$(\epsilon/k)_M$	10.22 K
σ_{A-M}	3.4873 Å
$(\epsilon/k)_{A-M}$	51.337 K
β_c	0.1
[He]	1.60896 10^{18} molecules
Z_{LJ}	4.6023 10^{-10} cm^3 molecule^{-1} s^{-1}
w	7.4044 10^7 s^{-1}

and the branching ratios α_j for all the different open channels j involved in the reaction are evaluated by:

$$\alpha_j = k_j(T)/k_{tot}(T) \tag{28}$$

B. ACIOSA/RRKM Model. In this second approach, justified in the beginning of section II, we used the result of a quasi-classical calculation of the capture rate constant, based on the Langevin model.[13,28] In this approach, the computed capture flux incorporates an implicit summation over the angular momentum J (this is the spirit of the capture theory). Hence, we have a microcanonical rate coefficient $k^{capture}(E)$ depending explicitly on the total energy E, not on J. To be consistent with the RRKM theory, we must introduce a distribution function $f(E)$ over which $k^{capture}(E)$ is to be averaged to lead to the thermal rate constant. We defined $f(E)$ as follows:

$$f(E) = \frac{\rho_r(E)e^{-E/k_BT}}{Q_r} \tag{29}$$

where $\rho_r(E)$ is the reactant density of states and $Q_r = Q_{CH}Q_{NO}$ is the partition function of reactants. To model the probabilities of passing over the various transition states encountered along the reaction paths, we defined the quantities $P_x(E,J)$ as the ratio of reactive flux to incident flux. According to Miller's unified statistical treatment,[16] $P_x(E,J)$ has the interpretation of an average reaction probability. If we consider the simple following scheme (Scheme 1)

SCHEME 1

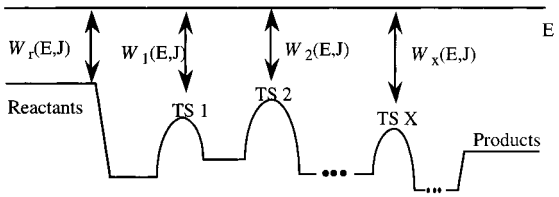

the probability of reactants to form a collision complex TS 1 is

$$P_1(E,J) = W_1(E,J)/[W_r(E,J) + W_1(E,J)] \tag{30}$$

the probability to passing over TS 2 is

$$P_2(E,J) = W_2(E,J)/[W_1(E,J) + W_2(E,J)] \tag{31}$$

and so on, until reaching the products

$$P_x(E,J) = W_x(E,J)/[W_{x-1}(E,J) + W_x(E,J)] \tag{32}$$

The quantities $W_x(E,J)$ represent the sum of states for fixed angular momentum J and $W_r(E,J)$ is related to reactants. All state-counting and convolution evaluations are done by the Beyer−Swinehart algorithm. The thermal rate constant $k_j(T)$ is then defined by the following quantity:

$$k_j(T) = \frac{1}{Q_r}\int dE\ \rho_r(E)k^{capture}(E)e^{-E/k_BT}\langle G_j(E,J)\rangle_J \tag{33}$$

with

$$G_j(E,J) = P_1(E,J)P_2(E,J)\ ...\ P_{x-1}(E,J)P_x(E,J) \tag{34}$$

and

$$\langle G_j(E,J)\rangle_J = \frac{\int dJ\ (2J+1)G_j(E,J)W(E,J)}{\int dJ\ (2J+1)W(E,J)} \tag{35}$$

It is necessary to include a suitable weight function in averaging of the branching ratios $G_j(E,J)$ over angular momentum, since the importance of the different J values depends on the rate at which the complex with these J values is formed. The rate at which complexes at different J values are formed is, of course, determined by the microcanonical capture flux, proportional to $(2J + 1)W(E,J)$. Hence, $(2J + 1)W(E,J)$ constitutes the correct weight function for the average in eq 35. We note that, for reactions of this type, it is important to compute the branching ratios explicitly as a function of *both E* and *J*, subsequently performing the thermal averaging, to take account of the different behaviors of the competing loose and tight transition states as a function of the angular momentum.

III. Results and Discussion

A. Total Rate Constant. The most recent experimental value of k_{tot}(300 K) has been obtained by Mehlmann et al.,[2i] using a combination of laser photolysis and laser induced fluorescence to measure the removal rate constants of CH and CD radicals in collision with NO at room temperature (see section I). They obtained k_{CH} (300 K) = (1.85 ± 0.10) × 10^{-10} cm^3 molecule^{-1} s^{-1} and k_{CD} (300 K) = (1.28 ± 0.18) × 10^{-10} cm^3 molecule^{-1} s^{-1}.

(i) CH + NO Reaction. The microcanonical variational calculation for the loose transition state associated with the RRKM treatment leads to a total rate constant k_{tot}(300 K) = 1.88 × 10^{-10} cm^3 molecule^{-1} s^{-1} in excellent agreement with experiment. Figure 3 presents an Arrhenius plot of the total rate coefficient for the CH + NO reaction determined by this approach in comparison with the available experimental data. The rate constant of disappearance of the reactants calculated with the μVTST/RRKM model is in good agreement at high temperatures with the experimental findings. Furthermore, as in all the experimental studies, we found no significant temperature dependence in the overall rate constant. The total rate constant predicted with the ACIOSA/RRKM model is k_{tot}(300 K) = 2.28 × 10^{-10} cm^3 molecule^{-1} s^{-1}, slightly higher than the μVTST/RRKM value. Such a situation is the consequence of a capture model which does not take into account recrossing effects and therefore overestimates the global rate constant. We can also pointed out the fact that the number of states $W(E,J)$ of the entrance channel, which appeared in formula 35, is calculated for an infinitely loose transition state by a standard RRKM theory, which is not totally consistent with the ACIOSA treatment of $k^{capture}(E)$ in formula 33. Hence, microscopic reversibility is not strictly obeyed in this ACIOSA/RRKM treatment. Conversely, the μVTST/RRKM calculations are fully consistent in this regard. However, this is in the spirit of the ACIOSA/RRKM approach, and since the computed k_{tot} lies in

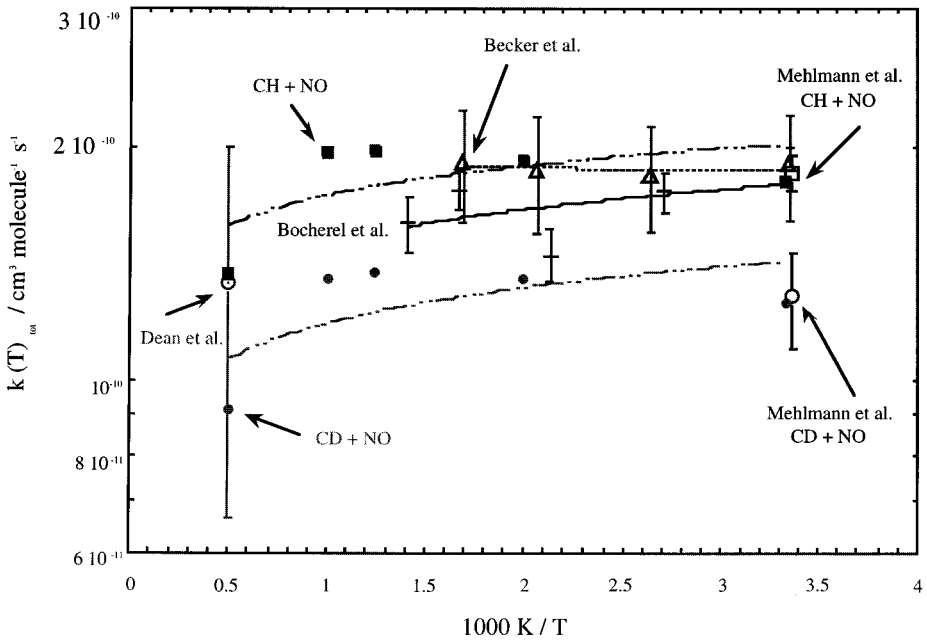

Figure 3. Comparison of the theoretical and experimental values of the second-order rate constant for the reaction CH + NO. The experimental data comes from different groups: (□) Mehlmann et al. for CH + NO,[2i] (○) Mehlmann et al. for CD + NO,[2i] (+) Bocherel et al.,[2h] (△) Becker et al.,[2g] (⊙) Dean et al.,[2e] (■) this work about CH + NO, and (●) this work about CD + NO. The lines are interpolation fittings using a function $k = AT^{-B}$.

TABLE 6: Calculated Values of the Total and Individual Rate Constants for the CH + NO Reaction as Function of Temperature[a]

T (K)	300	500	800	1000	2000
k_{HCN}	13.5	15.6	16.4	16.1	11.0
k_{HCO}	1.1×10^{-1}	3.2×10^{-1}	4.2×10^{-1}	5.1×10^{-1}	7.8×10^{-1}
k_{NCO}	2.6	2.9	2.6	2.4	1.5
k_{CO+NH}	1.5	1.4	1.4	1.4	0.9
k_{CN+OH}	0.3	0.1	0.1	0.1	7.3×10^{-2}
k_{CNO}	6.2×10^{-1}	4.1×10^{-1}	3.5×10^{-1}	3.0×10^{-1}	2.6×10^{-2}
k_{HNC+O}	1.6×10^{-2}	1.0×10^{-2}	1.0×10^{-2}	1.0×10^{-2}	8.2×10^{-3}
k_{HOC+N}	1.4×10^{-2}	7.0×10^{-3}	7.0×10^{-3}	6.8×10^{-3}	4.3×10^{-3}
k_{w_1}	1.7×10^{-1}	1.6×10^{-1}	1.4×10^{-1}	9.5×10^{-2}	7.3×10^{-2}
k_{w_2}	1.1×10^{-5}	8.2×10^{-6}	5.4×10^{-6}	4.2×10^{-6}	1.6×10^{-6}
k_{w_3}	1.1×10^{-8}	1.0×10^{-8}	9.1×10^{-9}	9.3×10^{-9}	8.2×10^{-9}
k_{w_4}	1.2×10^{-2}	1.4×10^{-2}	8.1×10^{-3}	6.6×10^{-3}	1.2×10^{-3}
k_{w_5}	1.2×10^{-6}	8.8×10^{-7}	5.8×10^{-7}	4.6×10^{-7}	1.8×10^{-7}
k_{w_6}	1.0×10^{-3}	7.4×10^{-4}	5.1×10^{-4}	4.1×10^{-4}	1.6×10^{-4}
k_{w_7}	1.2×10^{-8}	7.6×10^{-4}	5.7×10^{-4}	4.7×10^{-4}	1.8×10^{-4}
k_{tot}	18.8	20.9	21.4	20.9	14.6

[a] The rate constants are given in units 10^{-11} cm^3 molecule^{-1} s^{-1}, 50 Torr pressure is assumed to evaluate the stabilization rate constants k_{w_i}.

the same range as the domain of all the experimental values available for this reaction at 300 K, we shall not argue this point any further.

(ii) CD + NO Reaction. μVTST/RRKM calculations have also been performed on the reaction CD + NO. We obtain a total rate constant at room temperature for the deuterated reaction equal to $k_{tot}(300\ K) = 1.26 \times 10^{-10}$ cm^3 molecule^{-1} s^{-1}. The capture model gives for the same reaction $k_{tot}(300\ K) = 1.52 \times 10^{-10}$ cm^3 molecule^{-1} s^{-1}. These two values are consistent with the only experimental value available in the literature, the value proposed by Mehlmann et al.,[2i] that is to say, $k_{CD}\ (300\ K) = (1.28 \pm 0.18) \times 10^{-10}$ cm^3 molecule^{-1} s^{-1}.

B. Branching Ratios. The thermal rate constants obtained from the μVTST/RRKM approach for each product channel and for the stabilization of the intermediates involved in the CH + NO reaction are listed in Table 6. Table 7 presents the branching ratios calculated at room temperature by the μVTST/RRKM and ACIOSA/RRKM models for both reactions CH + NO and CD + NO.

(i) CH + NO Reaction. The μVTST/RRKM calculations indicate that all the collisional deactivation rate constants $k_{w_i}(T)$ associated with the intermediates i (Table 6) are negligible with respect to the rate constants of formation of the products. This is a consistent result since we deal with four atom intermediary species for which stabilization by collisions is rather weakly efficient. It turns out that all these rate constants are expected to be weakly pressure dependent. Comparisons between our results and the experimental data of Dean et al.[2e] and Okada et al.,[2f] presented in Table 1, are consistent since these authors do not propose accurate values but only tendencies. It is clear, as expected from most of the experimental reports and from the interpretation we suggested from the topology of the triplet potential energy surface (paper 1[12]), that O + HCN is the leading channel with a branching ratio around 72% with μVTST/RRKM and ACIOSA/RRKM approaches. About the other channels, the experimental determinations indicate a room-temperature branching ratio for CO + NH less than 10% for Dean et al. and less than 15% for Okada et al. We propose around 8%

TABLE 7: Theoretical Values of the Branching Ratios at 300 K for the Different Product Channels Involved in the Reactions (a) CH + NO and (b) CD + NO[a]

(a) CH + NO at 300 K	μVTST/RRKM	ACIOSA/RRKM
HCN + O	72.4%	65.3%
NCO + H	13.9%	14.9%
CO + NH	8.2%	11.1%
CNO + H	3.3%	5.3%
CN + OH	1.4%	2.5%
HCO + N	0.6%	0.8%
HNC + O	0.1%	0.1%
HOC + N	0.1%	0.1%

(b) CD + NO at 300 K	μVTST/RRKM	ACIOSA/RRKM
DCN + O, DNC + O	53.8%	51.2%
NCO + D, CNO + D	24.0%	23.9%
CN + OD	2.2%	4.6%
DCO + N, DOC + N, and CO + ND	20.0%	20.3%

[a] The calculations were performed using μVTST/RRKM and ACIOSA/RRKM approaches. For the CD + NO reaction, the channels CNO + D, DNC + O, and DOC + N, which play a minor role, have been grouped with their corresponding dominant parent channel.

TABLE 8: μVTST/RRKM Theoretical Branching Ratios (Information already Contained in Table 7a) Renormalized and Recast According to Bergeat Data[8] at Room Temperature

	if HCO and HOC are totally dissociated	if HCO and HOC are not dissociated	50% of HCO and HOC dissociated	experimental results of Bergeat et al. (from Table 2)
O atom	79.7%	80.2%	**79.9%**	**72.0 ± 10%**
H atom	19.6%	19.0%	**19.3%**	**21.0 ± 10%**
N atom	0.8%	0.8%	**0.8%**	**7.0 ± 3%**

with the μVTST/RRKM model and 11% with ACIOSA/RRKM. Lesser amounts are obtained for the CN + OH (1.4% with μVTST/RRKM and 2.5% with ACIOSA/RRKM) and HCO + N (less than 1%) product channels. These results are confirmed by the experimental findings, in which CN radicals are detected in very small amount.[2e,8]

Since Bergeat et al.[8] are able to give quantitative ratios for globally all the channels leading to the formation of a given atomic species, our results can be renormalized and recast in Table 8. Since we do not know the amount of dissociation of HCO which is expected to be only partial, an average situation evaluated between two extreme hypothesis (HCO totally dissociated into H + CO and HCO nondissociated) has been proposed like in the experimental study performed by Bergeat et al. The agreement between theory and experiment is still very satisfying compared to the experimental results collected in Table 2 and recalled in Table 8 for convenience. A slight discrepancy between theory (0.8%) and experiment (7%) is noted for the formation of N atoms. One argument to interpret it could be a possible missing direct dissociation channel toward HCO + N of the structure OC(N)H labeled D in paper 1[12] and presenting a star shape with the C atom in the center. If this hypothesis is confirmed theoretically (work in progress), it would increase substantially the amount of N atom formed and give a result in much better agreement with the experimental ratio of this channel.

(ii) CD + NO Reaction. Table 7b enable comparisons between our theoretical results for CD + NO and the values reported by Lambrecht et al.[7] at room temperature (Table 1). Once more, good agreements are obtained. It is clear that the major channel (i.e., the formation of DCN), plays a less dominant role relative to the hydrogenated parent reaction. It turns out that the rate constant for formation of DCN (and DNC) is roughly the same as the one of HCN. This can be interpreted

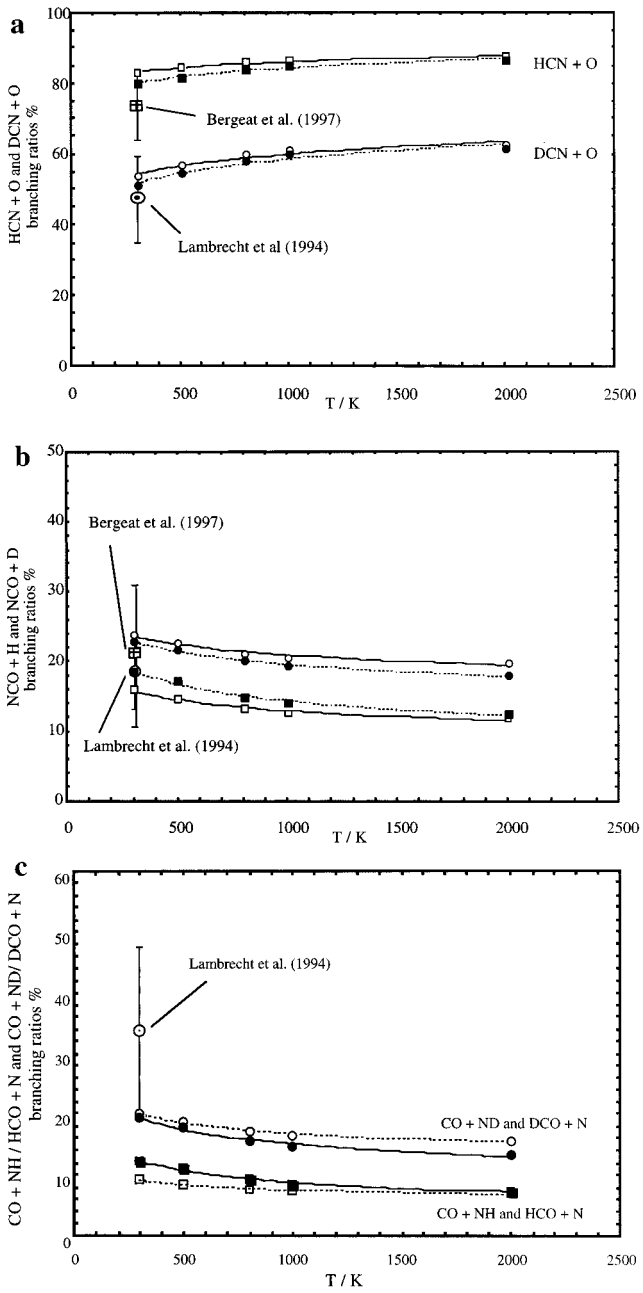

Figure 4. (a−c) Variation with temperature (in K) of the theoretical and experimental values of the branching ratios (in %) for the different product channels. The symbols used are the following: (⊙) are the experimental data from Lambrecht et al.,[7] (⊞) from Bergeat et al.,[8] (□) and (○) values are obtained with μVTST/RRKM approach, (■) and (●) values are obtained with the ACIOSA/RRKM approach. The circles (○) and (●) represented the calculations for CD + NO, (□) and (■) for CH + NO. In Figures 4b and 4c, a larger scale has been used for convenience.

by the fact that the CH bond is not significantly altered along the channel leading to HCN + O (see Figure 4a in paper 1[12]). Moreover, we expect that the sum and the density of states required to evaluate the microcanonical rate constants are modifyed in the similar manner by the isotopic effect along the pathway of formation of HCN + O. Conversely, the other channels are rather complex since they involve many steps in which the CH bond is involved. We can then predict that the isotopic effect will modify in different manners the sums of states of structures in which the C−H bond is elongated with respect to the density of states of structures associated with wells. Although it is difficult to go further than this simple

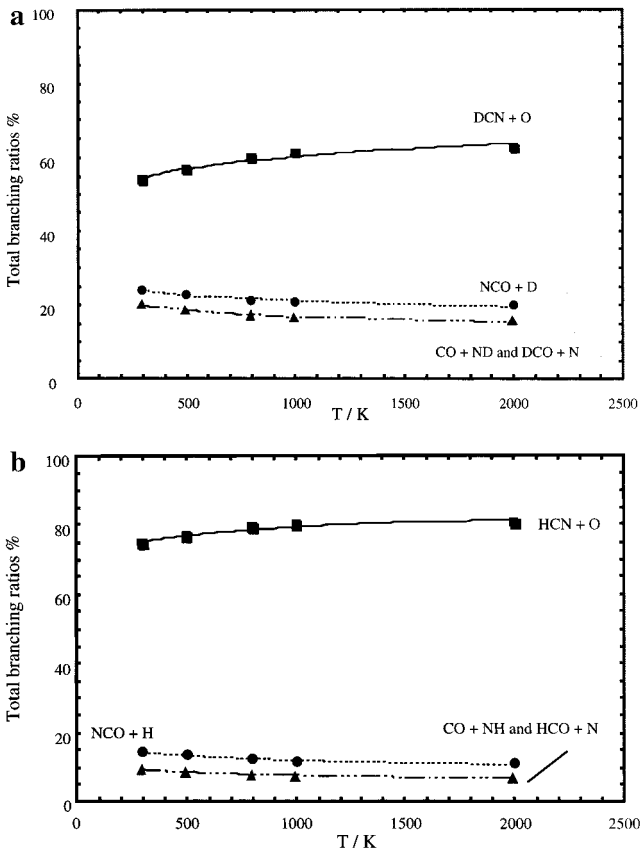

Figure 5. (a and b) Variation with temperature T (in K) of the theoretical branching ratios calculated with μVSTS/RRKM approach for each product channel of CD + NO (Figure 5a) and of CH + NO (Figure 5b).

interpretation of the change of the rate constant due to the isotopic effect, the net result is that all the other channels contribute to a global branching fraction larger than in the CH + NO parent process and consequently reduce the relative importance of the DCN + O channel. Our calculations indicate that the CO + ND and DCO + N product channels are less important than predicted by Lambrecht et al.: we obtain 20.0% with the μVTST/RRKM model and 20.3% with ACIOSA/RRKM, the experimental value being 33.7 ± 13.8%. However, some caveats to be borne in mind are discussed in the conclusion below.

(iii) Variation of the Rate Constants with Temperature. Figures 4 and 5 display the variation of some branching ratios of CH + NO and CD + NO reactions with temperature. Figures 4a, 4b, and 4c contain both theoretical and experimental results for CH + NO and CD + NO reactions. Figures 5a and 5b provide a global view of the variation with temperature of the most important branching ratios calculated for the deuterated species (Figure 5a) and hydrogenated species (Figure 5b). All the results agree about the weak temperature dependences of all these branching ratios. The agreement between theory and experiment is very satisfying.

IV. Concluding Remarks

The complexity of the topology of lowest triplet potential energy surfaces (PES) involved in the $CH(X^2\Pi) + NO(X^2\Pi)$ reaction emphasizes the level of the challenge for the theoretical determination of the branching ratios. The determination of the geometries, spectroscopic constants, and energies of the various stationary points (saddle points and minima) involved in the PES have been performed successfully by sophisticated ab initio calculations (see paper 1[12]). These data enables us to provide a reasonable estimation of the relative sums and densities of states (within the harmonic approximation) corresponding to these stationary points. Coupled with rather more sophisticated treatment of the barrierless entrance channel capture process (via μVTST or ACIOSA), this constitutes the crucial step in obtaining microcanonical rate constants. Both μVTST/RRKM and ACIOSA/RRKM give analogous global rate constants of disappearance of the reactants CH + NO and CD + NO, around 1.9×10^{-10} and 1.3×10^{-10} cm^3 molecule^{-1} s^{-1}, respectively at 300 K. These gas kinetics values are characteristic of processes governed by long-range forces.

Both methods give also similar branching ratios for the title reaction (i.e., HCN + O represents the dominant product channel), followed by NCO + H and CO + NH as predicted recently Bergeat et al.[8] and Lambrecht et al.[7] for the CD + NO reaction. The products CN + OH and HCO + N are observed in lesser amount as reported Dean et al.[2e] and Okada et al.[2f] The qualitative agreement between experiment and theory on the branching ratios is *a priori* promising. However, it should be noted that the theoretical strategy adopted here, involves several assumptions besides the harmonic force fields associated with each stationary point. First, these force fields have been determined at UHF/6-31G** level using the 0.89 magic factor proposed by Pople et al.[29] Second, we did not take into account any crossing between the triplet surface with the lowest singlet one. Moreover, some other crossings are expected to exist somewhere in the manifold of surfaces involved in this reaction. A possible extension of this work would be to investigate the role of such effects on the results. A short term objective will be the use of an analytical representation of the lowest singlet and triplet PES within the multivalued DMBE spirit[30] to get a more reliable determination of the density and sum of states free of any decoupled vibrational mode assumption. This work, and the work related to the possible direct decomposition of OC(N)H (structure D in paper 1[12]) into OCH + N discussed in section III.2.i), are in progress.

References and Notes

(1) (a) Miller, J. A.; Bowman, C. T. *Prog. Energy Combust. Sci.* **1989**, *15*, 287. (b) Strobel, D. F. *Planet. Space Sci.* **1982**, *30*, 839.

(2) (a) Butler, J. E.; Fleming, J. W.; Goss, L. P.; Lin, M. C. *Chem. Phys.* **1981**, *56*, 355. (b) Wagal, S. S.; Carrington, T.; Filseth, S. V.; Sadowski, C. M. *Chem. Phys.* **1982**, *69*, 61. (c) Berman, M. R.; Fleming, J. W.; Harvey, A. B.; Lin, M. C. *19th International Symposuim on Combustion*; The Combustion Institute: Pittsburgh, PA, 1982; p 73. (d) Lichtin, D.; Berman, M. R.; Lin, M. C. *Chem. Phys. Lett.* **1984**, *108*, 18. (e) Dean, A. J.; Hanson, R. K.; Bowman, C. T. *J. Phys. Chem.* **1991**, *95*, 3180. (f) Okada, S.; Yamasaki, K.; Matsui, H.; Saito, K.; Okada, K. *Bull. Chem. Soc. Jpn.* **1993**, *66*, 1004. (g) Becker, K. H.; Engelhardt, B.; Geiger, H.; Kurtenbach, R.; Wiesen, P. *Chem. Phys. Let.* **1993**, *210*, 135. (h) Bocherel, P.; Herbert, L. B.; Rowe, B. R.; Sims, I. R.; Smith, I. W. M.; Travers, D. *J. Phys. Chem.* **1996**, *100*, 3063. (i) Mehlmann, C.; Frost, M. J.; Heard, D. E., Orr, B.; Nelson, P. F. *J. Chem. Soc., Faraday Trans.* **1996**, *92*, 2335.

(3) Rieu, N−Q.; Henkel, C.; Jackson, J. M.; Mauersberger, R. *Astron. Astrophys.* **1991**, *241*, L33.

(4) Lindqvist, M.; Sandqvist, Aa.; Winnberg, A.; Johansson, L. E. B.; Nyman, L.-Å. *Astron. Astrophys., Suppl. Ser.* **1995**, *113*, 257.

(5) Bozzelli, J. W.; Dean, A. J. In *Combustion Chemistry*, 2nd ed.; Gardiner, W. C., Ed.; Springer-Verlag: Berlin, 1994.

(6) Takezaki, M.; Ohoyama, H.; Kasai, T.; Kuwata, K. *Laser Chem.* **1994**, *15*, 113.

(7) Lambrecht, R. K.; Hershberger, J. F. *J. Phys. Chem.* **1994**, *98*, 8406.

(8) Bergeat, A.; Loison, J. C.; Calvo, T.; Dorthe G. *Chem. Phys.* In press.

(9) Daugey, N.; Bergeat, A.; Caubet, P.; Schuck, A.; Dorthe, G. *News Lett. Anal. Astron. Spectrosc.* **1995**, *22*, 10.

(10) (a) Poppinger, D.; Radom, L.; Pople, J. A. *J. Am. Chem. Soc.* **1977**, *99*, 7806. (b) Yokoyama, K.; Takane, S.; Fueno, T. *Bull. Chem. Soc. Jpn.*

1991, *64*, 2230. (c) East, A. L. L.; Johnson, C. S.; Allen, W. D. *J. Chem. Phys.* **1993**, *98*, 2. (d) Pinnavaia, N.; Branley, M. J.; Su, M.; Green, W. H.; Handy, N. C. *Mol. Phys.* **1993**, *78*, 319.

(11) Mebel, A. M.; Luna, A. M.; Lin, C.; Morokuma, K. *J. Chem. Phys.* **1996**, *105*, 6439.

(12) Marchand, N.; Jimeno, P.; Rayez, J. C.; Liotard, D. *J. Phys. Chem.* **1997**, *101*, 6077.

(13) Marchand, N.; Stoecklin, T.; Rayez, J. C. To be submitted for publication.

(14) Bocherel, P.; Herbert, L. B.; Rowe, B. R.; Sims, I. R.; Smith, I. W. M.; Travers, D. *J. Phys. Chem.* **1996**, *100*, 3063.

(15) Diau, W.-G.; Smith, S. C. *J. Phys. Chem.* **1996**, *100*, 12349.

(16) Miller, W. H. *J. Chem. Phys.* **1976**, *65*, 2216.

(17) Wang, H.; Hase, W. L. *J. Am. Chem. Soc.*, **1997**, *119*, 3093.

(18) Wang, H.; Hase, L. W. *J. Am. Chem. Soc.*, **1995**, *117*, 9347.

(19) Klippenstein, S. *J. Chem. Phys.* **1996**, *104*, 5437.

(20) Chase, M. W.; Jr., Davies, C. A.; Downey, J. R.; Jr., Frurlp, D. J.; McDonald, R. A.; Syverud, A. N. *JANAF Thermochemical Tables, Journal of Physical and Chemical Reference Data*, 3rd ed.; American Chemical Society and the American Institute of Physics for the National Bureau of Standards; Washington, DC, 1985; Vol. 14.

(21) Gilbert, R. G.; Smith, S. C. *Theory of Unimolecular Recombinaison Reactions*; Blackwell Scientific Publication: Carlton, Australia, **1990**.

(22) (a) Smith, S. C. *J. Chem. Phys.* **1991**, *95*, 3404. (b) Smith, S. C. *J. Chem. Phys.* **1992**, *97*, 2406; Smith, S. C. *J. Phys. Chem.* **1993**, *97*, 7034. (d) Smith, S. C. *J. Phys. Chem.* **1994**, *98*, 6496.

(23) Wardlaw, D. M.; Marcus, R. A. *Adv. Chem. Phys.* **1988**, *70*, 231.

(24) Klippenstein, S. J. *J. Chem. Phys.* **1991**, *94*, 6469.

(25) Buckingham, A. D. *Advances in Chemical Physics*; Hirschfelder, J. O., Eds.; Interscience: New York, 1967; Vol. 9 (Permanent and induced molecular moments and long-range intermolecular forces), p 107.

(26) Troe, J. *J. Chem. Phys.* **1977**, *66*, 4745.

(27) Reid, R.; Sherwood, T. K. *The properties of Gases and Liquids—their Estimation and Correlation*, 2nd ed.; McGraw-Hill Book Company: New York, 1969.

(28) Davidsson, J.; Nyman, G. *Chem. Phys.* **1988**, *125*, 171.

(29) Hehre, W. J.; Radom, L.; Schleyer, P. v. R.; Pople, J. A. *ab initio Molecular Orbital Theory*; Wiley & Sons: New York, 1986.

(30) (a) Varandas, A. C. J. *Adv. Chem. Phys.* **1988**, *74*, 255. (b) Varandas, A. C. J. *Mol. Phys.* **1984**, *53*, 1303. (c)Varandas, A. C. J. *J. Mol. Struct.* (*THEOCHEM*) **1985**, *120*, 401. (d) Varandas, A. C. J.; Brandão, J.; Quintales, L. A. M. *J. Phys. Chem.* **1988**, *92*, 3732. (e) Prastrana, M. R.; Quintales, L. A. M.; Brandão, J.; Varandas, A. C. J. *J. Phys. Chem.* **1990**, *94*, 8073. (f) Varandas, A. C. J.; Voronin, A. I. *Mol. Phys.* **1995**, *95*, 497. (g) Varandas, A. C. J.; Pais, A. A. C. *Mol. Phys.* **1988**, *65*, 843. (h) Varandas, A. C. J. *Int. J. Quantum Chem.* **1987**, *32*, 563. (i) Varandas, A. C. J.; Pais, A. A. C. *Theoretical and Computational Models for Organic Chemistry*; Formosinho, S. J., Czismadia, I. G., Arnaut, L. G., Eds.; Kluwer: Dordrecht, 1991; p 55. (j) Jimeno, P.; Rayez, J. C.; Abreu, P. E.; Varandas, A. C. J. *J. Phys. Chem.* **1997**, *101*, 4828. (k) Varandas, A. C. J.; Yu, H. G. Double Many-Body Expansion Potential Energy Surface for Ground-State HO_3. In press. (l) Jimeno, P.; Rayez, J. C.; Abreu, P. E.; Varandas, A. C. J. To be submitted for publication.